PROCEEDINGS B

rspb.royalsocietypublishing.org

Research

Cite this article: Lecointe A, Domart-Coulon I, Paris A, Meibom A. 2016 Cell proliferation and migration during early development of a symbiotic scleractinian coral. *Proc. R. Soc. B* **283**: 20160206.
http://dx.doi.org/10.1098/rspb.2016.0206

Received: 29 January 2016
Accepted: 22 April 2016

Subject Areas:
cellular biology, developmental biology, environmental science

Keywords:
cell proliferation, BrdU, apoptosis, dinoflagellates, metamorphosis, scleractinia

Author for correspondence:
Isabelle Domart-Coulon
e-mail: icoulon@mnhn.fr

Electronic supplementary material is available at http://dx.doi.org/10.1098/rspb.2016.0206 or via http://rspb.royalsocietypublishing.org.

THE ROYAL SOCIETY PUBLISHING

Cell proliferation and migration during early development of a symbiotic scleractinian coral

Agathe Lecointe[1,2], Isabelle Domart-Coulon[2], Alain Paris[2] and Anders Meibom[1,3]

[1]Laboratory for Biological Geochemistry, School of Architecture, Civil and Environmental Engineering, École Polytechnique Fédérale de Lausanne (EPFL), Lausanne, Switzerland
[2]Unité MCAM UMR7245, Sorbonne Universités, Museum National d'Histoire Naturelle (MNHN), CNRS, Paris, France
[3]Center for Advanced Surface Analysis, Institute of Earth Sciences, University of Lausanne, Lausanne, Switzerland

In scleractinian reef-building corals, patterns of cell self-renewal, migration and death remain virtually unknown, limiting our understanding of cellular mechanisms underlying initiation of calcification, and ontogenesis of the endosymbiotic dinoflagellate relationship. In this study, we pulse-labelled the coral *Stylophora pistillata* for 24 h with BrdU at four life stages (planula, early metamorphosis, primary polyp and adult colony) to investigate coral and endosymbiont cell proliferation during development, while simultaneously recording TUNEL-positive (i.e. apoptotic) nuclei. In the primary polyp, the fate of BrdU-labelled cells was tracked during a 3-day chase. The pharynx and gastrodermis were identified as the most proliferative tissues in the developing polyp, and BrdU-labelled cells accumulated in the surface pseudostratified epithelium and the skeletogenic calicodermis during the chase, revealing cell migration to these epithelia. Surprisingly, the lowest cell turnover was recorded in the calicodermis at all stages, despite active, ongoing skeletal deposition. In dinoflagellate symbionts, DNA synthesis was systematically higher than coral host gastrodermis, especially in planula and early metamorphosis. The symbiont to host cell ratio remained constant, however, indicating successive post-mitotic control mechanisms by the host of its dinoflagellate density in early life stages, increasingly shifting to apoptosis in the growing primary polyp.

1. Introduction

Scleractinian corals are evolutionary ancient marine animals that build large reef structures in (sub-)tropical coastal waters, providing habitats for extremely diverse marine ecosystems [1]. The reefs are constructed through accumulation of aragonitic exoskeleton produced by the polyps, which are the fundamental physiological unit of scleractinian corals. The polyps host endosymbiotic photosynthetic dinoflagellates that strongly boost skeletal production [2]. However, the cellular processes initiating and driving skeletogenesis and controlling the density of *Symbiodinium* sp. endosymbionts remain obscure in both adult colonies and early life stages, which are critical to coral recruitment and reef survival. Studies on tissue homeostasis in scleractinians have mostly focused on the vulnerability of adults and their dinoflagellates to environmental stress, which can lead to symbiont loss and tissue bleaching (reviewed in [2] and [3]). Processes of cellular turnover, which include cell proliferation, migration and death, have hardly been investigated, and sparse existing work has focused on adult corals. Indeed, it was shown that colonies undergo apoptotic death in response to increased temperature and reduced pH [4,5], or changes in proliferation during disease and lesion repair [6,7]. Baseline levels of coral and dinoflagellate cell proliferation were recently experimentally determined at tissue scale in polyps from adult *Pocillopora damicornis* coral colonies, pulse-labelled for 24 h with BrdU [8].

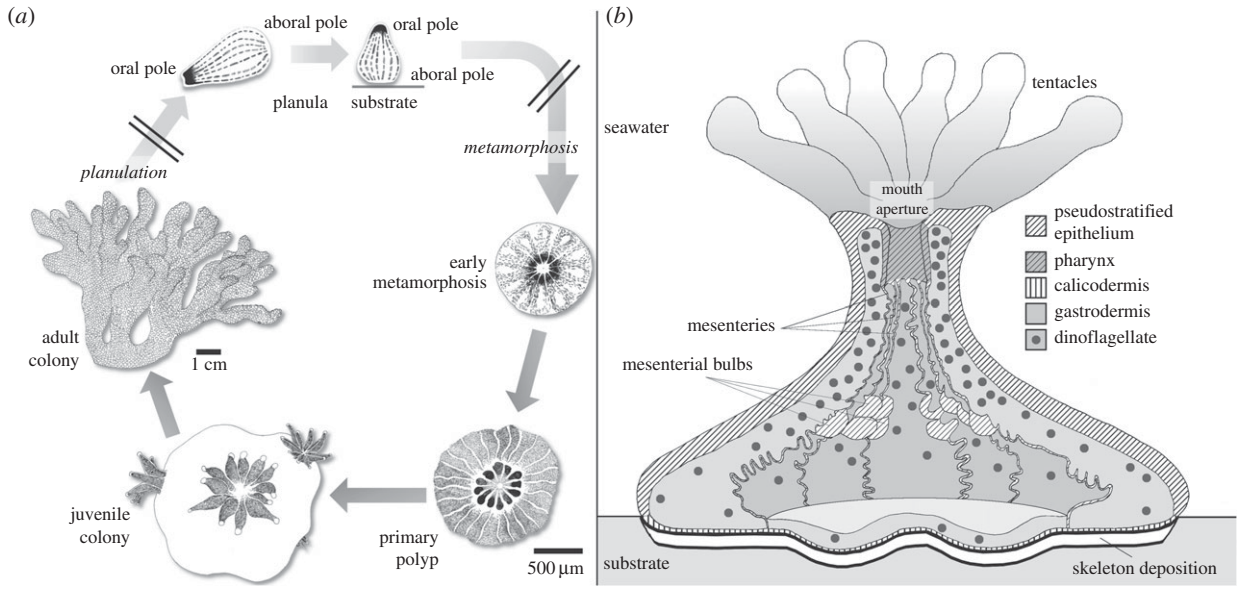

Figure 1. Tissue organization during *Stylophora pistillata* metamorphosis. (*a*) Coral cycle of development. The planula probes the substrate with its oral pole and, upon reception of suitable cues, flips over and flattens into a disc with its aboral pole pressed against the substrate, characteristic of the 'early metamorphosis' stage. Complete metamorphosis leads to the primary polyp stage, with tentacles budding around the mouth aperture, lateral spreading of the tissue and vertical extension of the body column. (*b*) Tissue structures in the primary polyp. Oral tissue, facing the seawater, is composed of a relatively thick bilayer of pseudostratified epithelium (pse, also called epidermis), with oral gastrodermis lining the gastric cavity. The mouth in the centre of the oral disc is connected to a ring of upward growing tentacles, while the pharynx grows inward and connects with radial mesenteries. Aboral tissue, facing the skeleton, is composed of a thin bilayer of calicodermis (skeletogenic tissue) and aboral gastrodermis. Dinoflagellate symbionts are hosted in the gastrodermal cells. Epithelial bilayers are separated by mesogleal gel.

However, early life stages offer the unique opportunity to investigate the ontogeny of morphogenetic processes in each specialized coral tissue, particularly with respect to the skeleton-forming calicodermis, and the host regulation of its *Symbiodinium* endosymbiont density.

The life cycle of a colonial reef-building scleractinian coral is illustrated in figure 1*a*, for species with internal fertilization, such as *Stylophora pistillata* (Esper, 1797), which releases swimming planktonic planula larvae from the brooding colony [9]. Metamorphosis-induced morphogenetic tissue changes enable the coral to rapidly initiate skeletal deposition [10,11]. Within 2–4 days, the primary polyp is fully functional and continues to grow vertically and horizontally (illustrated in figure 1*b*). Within 6–12 days, secondary polyps start to bud at the periphery of the primary polyp, forming a juvenile colony.

In this study, we evaluated cell turnover, by which we mean proliferation, migration and death (by apoptosis), in each forming epithelium during planula larval metamorphosis into primary polyp, permitting us to (i) identify reservoirs of high proliferation activity, (ii) infer cell migration patterns and (iii) quantitatively investigate the ontogeny of coral host control over its dinoflagellate symbiont density.

2. Material and methods

(a) Biological material

Planula larvae of *S. pistillata* were collected at approximately 5 m depth in May 2013 from 7 to 11 parent colonies (greater than 30 cm width), on the reef of the Inter-University Institute for Marine Sciences, 5 km south the Coral Nature Reserve of Eilat, Israel, under permit number 2011/38182. Shallow-water (2–6 m) *S. pistillata* from the Gulf of Eilat contain clade A *Symbiodinium* sp., both at planula and adult colony stages [12]. Actively swimming planulae were distributed in batches of 10 larvae in 10 ml seawater in plastic dishes (lumox Sarstedt, or classic Petri dishes, 5 cm diameter), fitted with underwater paper that had been exposed for 5 days to natural seawater to initiate biofilm formation. Dishes were incubated in shaded outdoor running seawater tables, at 23–25°C, with seawater renewal every 6 h. Inorganic nutrient concentrations at the seawater surface and 20 m depth, obtained for the week of the experiments from the Israel National Monitoring Program at the Gulf of Eilat (http://www.iui-eilat.ac.il/Research/NMPmeteodata.aspx), were 0.014–0.018 µM NH_4, 0.007–0.011 µM NO_2, 0.04–0.36 µM NO_3 and 0.023 µM PO_4, corresponding to an oligotrophic environment. Salinity was 40.7‰, pH 8.17 and oxygen 218.5–219.9 µM. Ambient daylight intensity of approximately 500 µEinstein m^{-2} s^{-1} was measured at the water surface at midday with a LI-CORE 1000 Data Logger radiometer, corresponding to attenuation of direct sunlight by a factor three. Asynchronous larval metamorphosis and polyp development were monitored under the binocular microscope (5×) during 6 days. Replicates of each of three different early life stages, identified by their morphogenetic features, were collected: planula, early metamorphosis and primary polyp (figure 1*a*). Small colonies (less than 1 cm width and 0.5 cm tall), spontaneously settled in the outdoor seawater tables about two months earlier from another batch of *S. pistillata* planulae, were used as control adult life stage.

(b) BrdU pulse-chase labelling to detect DNA synthesis and cell turnover

Cell proliferation during larval metamorphosis and primary polyp development was assessed using the BrdU (5-bromo-2′-deoxyuridine) labelling method, slightly modified from [8,13]. Larvae or recruits were incubated for 24 h at selected developmental stages in seawater containing 50 µM BrdU (Roche), renewed every 6 h. Corresponding unlabelled controls were incubated in normal seawater without BrdU. At the end of the 24 h pulse, three to five individual replicates and their corresponding controls were sampled for each life stage. Among the primary

polyps pulse-labelled with BrdU for 24 h, a few individuals were allowed to further grow in running seawater for a chase period of 48 h (two replicates; the third was lost) or 64 h (three replicates).

(c) Serial tissue sectioning

At the end of the BrdU pulse or the chase, samples were fixed overnight at 4°C and prepared for serial sectioning following procedures detailed by Lecointe *et al.* [8]. Unicryl (EMS)-embedded samples were cut into semi-thin sections (1 µm thick) with a 35° diamond knife (Diatome) on an Ultracut microtome, at the MNHN PtME platform of electron microscopy (Paris). Serial sets of sections, obtained at three separate depths in each replicate, were used for (i) histological staining with toluidine blue-basic fuschin (EMS) for identification and orientation in the larval/polyp structure, (ii) BrdU immunolocalization and (iii) apoptosis detection by terminal transferase-mediated dUTP nick end labelling (TUNEL) assay.

(d) Immunolocalization of BrdU-labelled nuclei

The BrdU-labelling index measures the proportion of cell nuclei having incorporated BrdU in their newly synthesized DNA during the 24 h pulse. BrdU was immunodetected in tissue sections with primary anti-BrdU mouse antibody (Roche) and Alexa-594-labelled secondary goat anti-mouse antibody (Invitrogen), and nuclei were counterstained with DAPI (Invitrogen), following [8]. Sections were observed on a wide-field fluorescence microscope (Olympus XM10 slide scanner) at the EPFL PT-BIOP platform (Lausanne) using DAPI (Ex 377/50 nm, Em 440/40 nm), and CY3 filters (Ex 560/25 nm, Em 607/36 nm) at spatial lateral resolution of approximately 0.5 µm. A total of four to eight sections were imaged for each of three to five biological replicates per life stage, and analysed with ImageJ software (v. 1.49) using the cell counter plug-in to manually count BrdU-labelled nuclei among DAPI-counterstained total nuclei (for method, see electronic supplementary material, figure S1). Labelled nuclei were not detected in control tissue unexposed to BrdU (one negative control examined per life stage). Totals of 345–64 810 nuclei were counted per tissue type (depending on section orientation).

Dilution of BrdU labelling intensity was quantified during the 3 days chase in seawater. Dilution is caused by de novo synthesis of unlabelled DNA, through entry of cycling cells into S phase and division. An intensity drop by a factor of two can thus be attributed to one cell division. During the chase experiment, the fluorescent signal intensity of labelled nuclei was measured for BrdU and DAPI, background was substracted and the CY3/DAPI signal intensity ratios were compared ($n = 30–60$ nuclei per tissue type, per chase time-point).

(e) Tunel assay for detection of apoptotic cell nuclei

Apoptosis was evaluated in the same biological samples previously analysed for BrdU labelling, using serial sections at similar depths in the tissue. Control samples not exposed to BrdU were also assessed for apoptosis (one control per life stage). Apoptosis is characterized by formation of DNA breaks (nick), and the TUNEL reaction uses the enzyme terminal deoxynucleotidyl transferase (TdT) to fill these gaps with fluorescein (FITC)-labelled dUTP. The TUNEL assay was performed for 1 h at 37°C according to kit instructions (*in situ* cell death detection—fluorescein, Roche). For negative controls, TdT enzyme was omitted from the reactive solution. For positive controls, sections were pre-incubated with recombinant DNAse I (3 U ml^{-1}, Ambion) for 10 min at room temperature. Treated sections were mounted with Prolong Gold Antifade reagent with DAPI (Invitrogen) and observed on a wide-field fluorescence microscope (Olympus XM10 slide scanner, PT-BIOP, EPFL), using DAPI (Ex 377/50 nm, Em 440/40 nm) and FITC filters (Ex 485/20 nm, Em 525/30 nm), at spatial lateral resolution of approximately 0.3 µm. The proportion of TUNEL-positive cell nuclei was calculated from acquired images, using the counter cell plugin from ImageJ software. For each life stage, three biological replicates were assessed, with one to four sections imaged per replicate, and totals of 657 to 8219 nuclei counted per tissue type (depending on section orientation).

(f) Mitotic index and abundance of dinoflagellates

For the endosymbiotic dinoflagellates, the mitotic index was calculated as the ratio of the number of dinoflagellate doublets (undergoing cytokinesis) to single dinoflagellate cells [14], in toluidine blue-stained sections of three replicates for each life stage (two to eight sections per replicate and 1200–2000 dinoflagellates counted per life stage). Results are presented as the mean $\pm$ 1 s.d. of doublet-to-single dinoflagellate ratio, for three biological replicates per life stage.

Dinoflagellate abundance (i.e. the number of symbiont nuclei relative to coral cell nuclei within the gastrodermal host tissue) was calculated using DAPI-stained nuclei counts previously obtained for assessment of the BrdU-labelling index (electronic supplementary material, table SI). Results are presented as mean $\pm$ 1 s.d. for three to five biological replicates per life stage.

(g) Statistical analyses

Fluorescence images, acquired from BrdU and TUNEL assays in semi-thin sections at three different depths in each replicate sample, allow visualization of labelled or unlabelled nuclei according to tissue type. The data follow a binomial distribution with uneven variance and were statistically analysed using the generalized linear model (GLM) using the binomial family and logit link function in R software v. 3.2.0. Significance was assessed at $\alpha = 0.05$ threshold p-value. Quantitative data for BrdU and TUNEL labelling are presented as boxplots, also reporting the means (as a cross) and outliers (detected outside the 1.5$\times$ inter-quartile range). The CY3/DAPI signal intensity ratio does not follow a normal distribution, as cells are not synchronous and the quantity of BrdU incorporated into the DNA is time-dependent (during the 24 h pulse, a cell ending the S-phase will incorporate less BrdU than a cell that is just starting DNA replication). Therefore, non-parametric Kruskal–Wallis tests were used, followed by pairwise Wilcoxon's test when significant. For dinoflagellate mitotic index and abundance, the normality of residues and homoscedasticity of data allowed application of one-way ANOVA followed by Tukey HSD tests.

3. Results

(a) Tissue organization and remodelling during metamorphosis

Major changes in tissue structure occur during coral lifestyle transition from swimming planula to sessile polyp, illustrated in figure 2 for four life stages: planula larva, early metamorphosis, primary polyp and adult polyp. The larval single bilayer of epithelia—pseudostratified epithelium (pse) and lipid-filled gastrodermis (g)—transforms into the polyp double bilayer of epithelia. Specialized areas connected to the surface pse develop from the larval oral and aboral poles during metamorphosis. The skeletogenic calicodermis (cal) differentiates in the basal floor at the interface with the

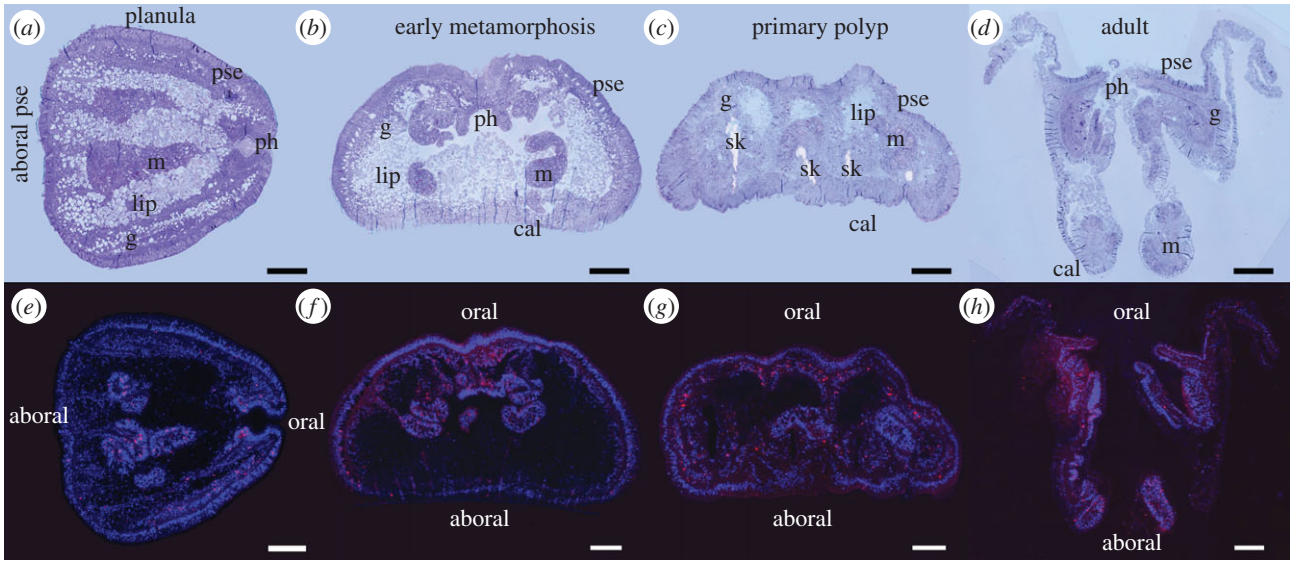

Figure 2. Distribution of BrdU-labelled nuclei in coral tissue from planula to adult polyp. (*a–d*) Toluidine blue-stained (1 µm) tissue sections. (*e–h*) BrdU-positive nuclei immunodetected with Alexa-594 fluorochrome (red) among nuclei counterstained with DAPI (blue). Scale bars, 100 µm; pse, pseudostratified epithelium; ph, pharynx; g, gastrodermis; m, mesentery; cal, calicodermis; lip, lipids; sk, skeleton.

substrate, and the pharynx (ph) forms by inward invagination of the pse, just below the oral disc. Tentacles grow upward from the oral disc (figure 1*b*; electronic supplementary material, figure S1; not visible in figure 2 in the sections selected), but were not studied here because they retracted upon fixation, and thus were hard to distinguish from inner mesenterial bulbs (or cnidoglandular bands [15]), which were therefore also not included in this study (figure 1*b*).

The inner gastrodermis, lining the digestive cavity, forms a continuous epithelium from oral to aboral pole in the larva, and connects the oral disc with the basal floor in the polyp (figures 1*b* and 2*a–d*). The gastrodermis contains intracellular symbiotic dinoflagellates, which are more abundant in oral compared with aboral areas (figure 1*b*). Mesenteries, already present in this species at the planula stage, are radial inward-growing tissue folds attached below the pharynx and composed of gastrodermis and a thin layer of pse, forming radial partitions of the gastric cavity. In the polyp, these mesenteries connect the pharynx to the edges of the basal floor (figure 1*b* and figure 2*a–d*).

(b) Coral cell proliferation and apoptosis

The spatial distribution of dividing cells, in the S phase of DNA synthesis (and thus labelled with BrdU during the 24 h pulse), is illustrated for each tissue structure and developmental stage in figure 2*e–h*, and electronic supplementary material, figure S1*b–e*, where BrdU is immunodetected (in red) among the DAPI-counterstained nuclei (in blue). Labelled nuclei were not detected in control tissue unexposed to BrdU (data not shown). Cell proliferation was found to be spatially and temporally highly heterogeneous, with scattered distribution of BrdU-positive nuclei, at densities depending on cell type and coral life stage.

The proportion of BrdU-positive nuclei is summarized for each tissue and developmental stage (figure 3*a–d*), along with the proportion of apoptotic nuclei, positive for the TUNEL enzymatic assay (figure 3*e–h*). Data are presented for the pharynx, pse and calicodermis, which share a common ectodermal origin, and for the gastrodermis, of endodermal origin. No significant differences were observed between oral and aboral gastrodermis, so these data were pooled. In planulae and early metamorphosis, less than 3% of coral cells from all three epithelia of ectodermal origin synthesized DNA within the 24 h pulse period, while in the gastrodermis up to 6% of the cells were BrdU-positive (figure 3*a–d*). However, in developing primary polyps, a peak of BrdU labelling was observed in the pharynx ($19.3 \pm 7.3\%$) together with a significant increase in BrdU labelling of the gastrodermis ($11.1 \pm 6.7\%$). Interestingly, this sudden increase in proliferation was not observed in other areas of the developing primary polyp, such as the pse, or the calicodermis (despite active, ongoing skeleton deposition; see electronic supplementary material, figure S2). In adult polyps, BrdU labelling strongly decreased compared with in the primary polyp, in both pharynx (by a factor 4) and gastrodermis (by a factor 3), whereas it increased (by a factor 2) in the pse ($7.3 \pm 1.6\%$). In adult polyps, the pse and the pharynx are the most proliferative tissue types, with $7.3 \pm 1.6\%$ and $5.5 \pm 2.0\%$ BrdU-labelled nuclei during the 24 h pulse, respectively, whereas the calicodermis remains the least proliferative tissue (figure 3*a–d*; electronic supplementary material, table SI).

The number of TUNEL-positive, apoptotic nuclei did not increase in sections of tissue exposed to BrdU compared with control tissue unexposed to BrdU, indicating no effect of the BrdU-labelling protocol on apoptosis (data not shown). Globally, in all three epithelial tissues of ectodermal origin, the relative abundances of TUNEL-positive nuclei were lower than BrdU-positive nuclei, with less than 1% of apoptotic cells counted in the pse, less than 2% in the calicodermis and a maximum of 2.5% in the pharynx of primary polyps, and non-significant differences between life stages (figure 3*a–c* and *e–g*; electronic supplementary material, table SII). In the gastrodermis, however, TUNEL labelling of nuclei was higher, at $3.3 \pm 2.2\%$ in planulae, reaching $5.1 \pm 2.4\%$ during early metamorphosis, and then decreasing in primary polyps, to below 2% in adults (figure 3*d*,*h*; electronic supplementary material, table SII).

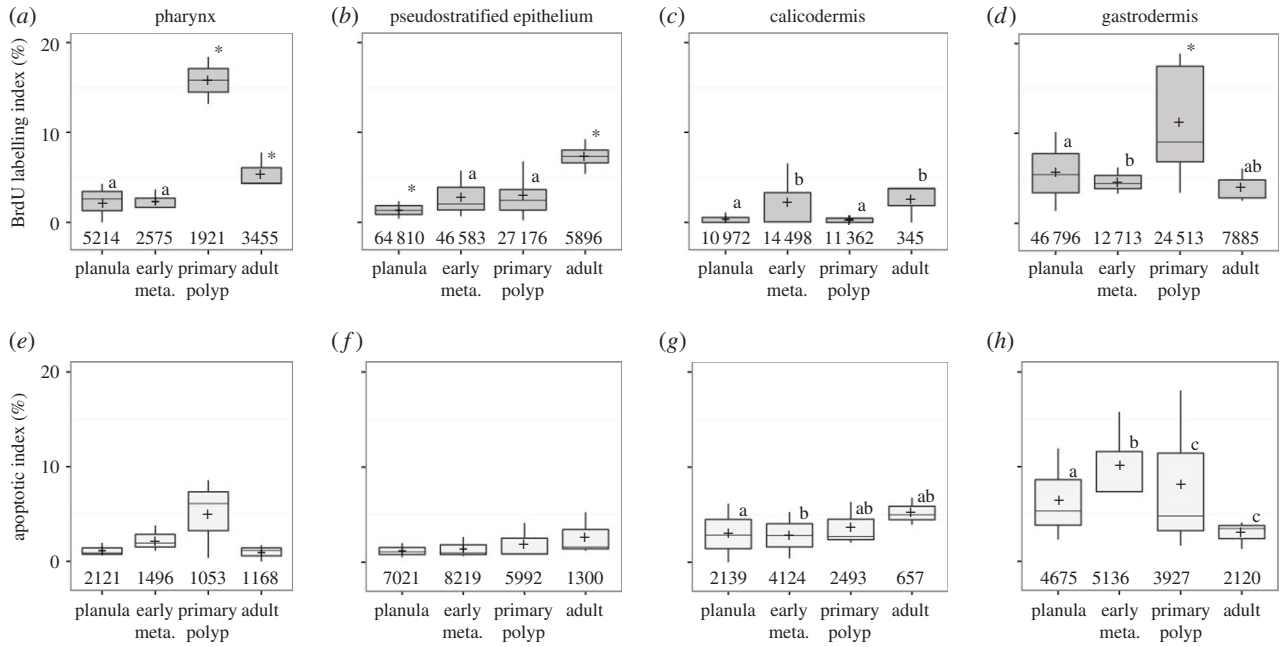

Figure 3. Tissue-specific cell turnover during metamorphosis. (*a–d*) BrdU-labelling index at the end of the 24 h pulse. (*e–h*) Apoptotic index in corresponding serial tissue sections of the same samples. In planula, the 'calicodermis' is not yet differentiated and this term refers to the aboral pse. Early meta., early metamorphosis. Data are expressed as boxplots, with the average visualized as +, and total nuclei counts reported above the *x*-axis. An asterisk indicates significant differences with other averages. Significantly different groups are labelled with different letters (GLM, $p < 0.05$).

(c) Coral cell movements in the ectoderm-derived epithelia

The fate of BrdU-labelled cells was monitored at the primary polyp stage during a 64 h chase period in normal seawater, allowing tracking of labelled cells in the developing epithelia, particularly in the pharynx, the pse and the calicodermis of the growing primary polyp (figure 4*a*,*c*,*e*). Accumulation or depletion of BrdU-labelled cells in specific tissue structures provide indirect evidence for cell import or loss, through cell death or export to other areas. De novo cell cycling in normal seawater dilutes the BrdU signal intensity because BrdU-labelled cells synthesize new, non-labelled DNA before division. The patterns of coral cell movements were thus recorded in these three connected epithelia in order to investigate the origin and turnover of cells in the skeletogenic calicodermis. All data are provided in electronic supplementary material, tables SIII and SIV.

At the beginning of the chase, the pharynx of the primary polyp was highly BrdU-labelled ($19.3 \pm 7.3\%$) compared with the pse ($2.9 \pm 2.5\%$) and calicodermis ($0.4 \pm 0.4\%$). At 48 h into the chase, the proportion of BrdU-labelled nuclei remained stable in the pharynx ($19.8 \pm 4.4\%$), whereas it increased by fivefold and sevenfold in the pse ($15.6 \pm 5.7\%$) and calicodermis ($2.9 \pm 2.5\%$), respectively. At 64 h into the chase, the BrdU-labelling index had significantly decreased in the pharynx ($11.4 \pm 6.6\%$), and returned to the initial low levels seen at the beginning of the chase in both pse and calicodermis (figure 4*a*,*c*,*e*).

At 48 h into the chase, a twofold dilution of the BrdU signal intensity was observed in both pharynx and pse, indicating division of BrdU-positive cells, whereas a similar decrease was difficult to detect in the calicodermis, in part due to high signal heterogeneity and lower initial BrdU-labelling levels (figure 4*b*,*d*,*f*).

(d) Dinoflagellate cell turnover in the coral host gastrodermis

Comparative dynamics of cell proliferation and apoptosis in endosymbiotic dinoflagellates and coral gastrodermis are presented in figure 5, along with the evolution of dinoflagellate mitotic index and relative dinoflagellate abundances. All data are provided in electronic supplementary material, tables SI, SII and SV.

Rates of BrdU-labelled nuclei were systematically two to five times higher in endosymbiotic dinoflagellates than in host gastrodermis in all three early life stages (GLM analysis, $p < 0.05$; figure 5*a*). In adult polyps, DNA synthesis was also twice as high in endosymbionts as in the host. High variability of the BrdU signal in dinoflagellates indicates spatial heterogeneity and asynchronous cell cycling during the 24 h pulse. No significant differences were observed for dinoflagellates between oral and aboral tissue, however. The mitotic index of dinoflagellates (representing a snapshot of the frequency of dinoflagellate doublets, i.e. visible mitotic figures at the time of tissue fixation) was lower than 2.5% at all stages, except in the primary polyp where it reached $6.3 \pm 2.3\%$ (figure 5*b*). Owing to their small size, the mitotic index of coral cells could not be accurately estimated.

Higher apoptotic indices were observed for dinoflagellates than gastrodermis in planulae and at early metamorphosis (about 11–12% versus 3–5%, respectively). However, in primary polyps, apoptosis of dinoflagellates rose dramatically (up to 35%) compared with coral cells (approx. 4%). In adult polyps, apoptosis of the endosymbionts remained high at approximately 28% versus less than 2% for the gastrodermis (figure 5*c*; electronic supplementary material, table SII).

Interestingly, the dinoflagellate relative abundance (ratio of symbiont to host nuclei in the gastrodermis) remained stable throughout metamorphosis, at about 5–10% (one-way

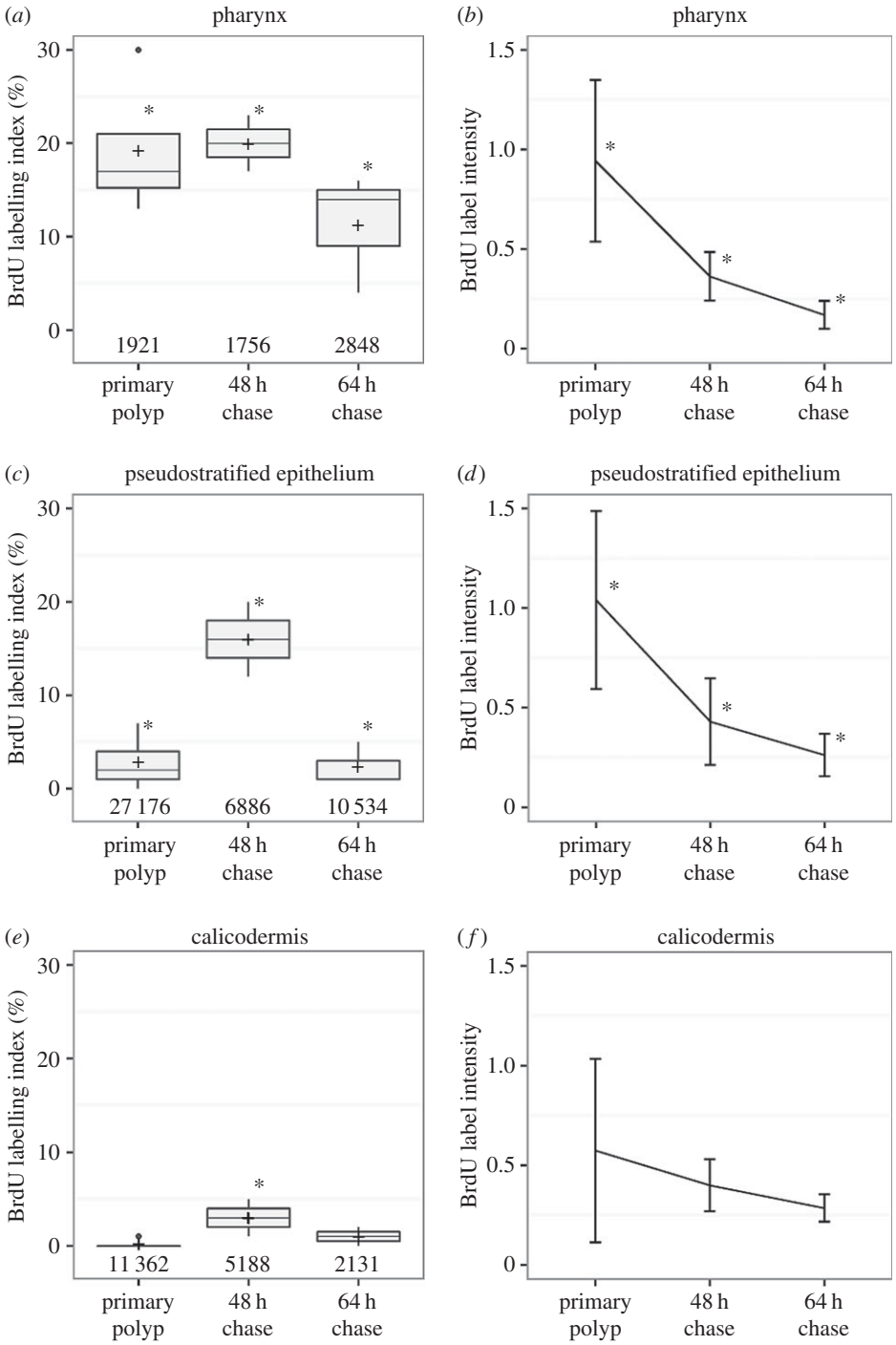

Figure 4. Chase of the BrdU label in the ectoderm-derived epithelia. (*a*,*c*,*e*) BrdU-labelling index in the primary polyp at the start, and 48 h and 64 h into the chase in normal seawater, respectively. Data are expressed as boxplots. An asterisk indicates a significantly different average from all other time points (GLM, $p < 0.05$). (*b*,*d*,*f*) Dilution of the BrdU signal intensity. An asterisk indicates significant differences with other averages (Kruskal–Wallis and pairwise Wilcoxon test, $p < 0.05$).

ANOVA, $p = 0.2$; figure 5*d*), indicating a series of post-mitotic control mechanisms by the host of its endosymbiont population with an increasing role for apoptosis in the developing primary polyp.

During the chase in normal seawater, the proportion of BrdU-labelled dinoflagellate symbionts remained stable at 20–25% in the growing primary polyp, with very slow dilution of BrdU (significant only at 64 h; electronic supplementary material, figure S3*a* and table SIII), indicating decreased dinoflagellate division. By contrast, the combined depletion by a factor of 3 of BrdU-labelled gastrodermal cells and their corresponding BrdU signal dilution at the end of the chase (electronic supplementary material, figure S3*b*,*c*) indicate active cell division in the host gastrodermis. Taken together, these results indicate decreasing cycling of endosymbiont cells relative to host cells in the growing primary polyp.

4. Discussion

This work presents the first detailed assessment of cellular turnover at tissue scale during developmental morphogenesis in a scleractinian coral, and reveals the ontogenetic flexibility of its dinoflagellate-host density regulations. Cellular morphogenetic processes have mostly been characterized in Cnidaria during regeneration or development of medusozoans, such as freshwater *Hydra* and marine *Hydractinia* [16–18]. Proliferating cells from adult anthozoans, pulse-labelled

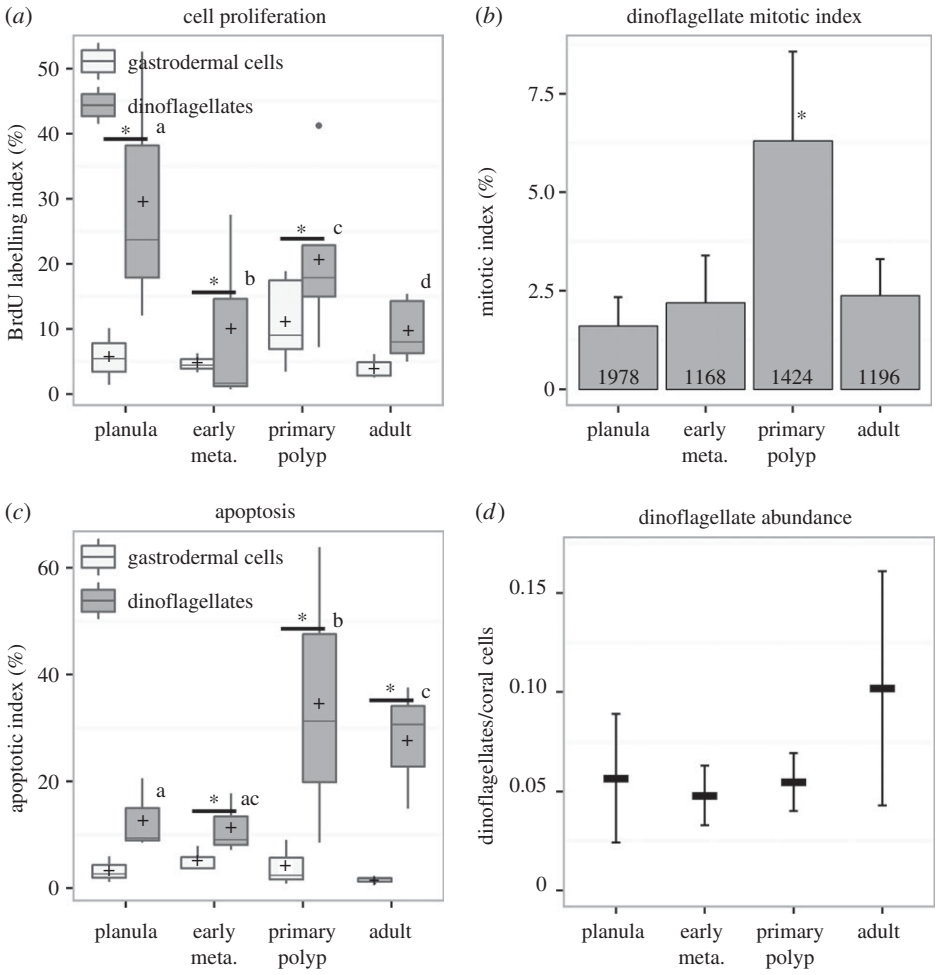

Figure 5. Dinoflagellate turnover in host gastrodermis during metamorphosis. (*a*) BrdU-labelling index in the gastrodermis after the 24 h pulse, for the dinoflagellates (dark grey) and the coral cells (light grey). An asterisk indicates a significant difference between dinoflagellates and gastrodermis (GLM, $p < 0.05$). (*b*) Mitotic index of dinoflagellates. The asterisk indicates a significant difference with all other stages (Tukey HSD, $p < 0.05$). (*c*) Apoptotic index in serial tissue sections of the same samples. An asterisk indicates a significant difference between dinoflagellates and gastrodermal cells. (*d*) Dinoflagellate relative abundance in the gastrodermis: no statistical differences were detected between stages (one-way ANOVA, $p = 0.697$). Early meta., early metamorphosis.

with thymidine analogue EdU or BrdU, were monitored during wound-regeneration and post-bleaching recovery in oral tissue of sea anemones [19,20], and during growth anomaly disease in *Porites* or *Montipora* corals [7]. However, the spatial and temporal dynamics of cell proliferation, migration and death have never been investigated in the developing calcifying scleractinians. Larval metamorphosis requires extensive tissue remodelling to establish the primary polyp structures. Here, we quantify the cell turnover in each forming scleractinian coral epithelium, and the symbiont-to-host cell ratio, from initiation of larval metamorphosis to the fully developed primary polyp.

(a) Identification of the pharynx as a hotspot of coral cell turnover during development

At the end of the 24 h BrdU pulse, a comparison of labelling levels between tissues from all life stages reveals enhanced coral cell proliferation in the primary polyp, with a hotspot of DNA synthesis localized in the pharynx (figure 3*a*). This specialized epithelium of ectodermal origin is the most productive tissue area, with up to 19% of cells undergoing DNA synthesis in the primary polyp, and low rates of cell death by apoptosis (less than 2.5%). In the rest of the pseudostratified epithelium (pse), DNA synthesis rates vary from less than 3% in early life stages to 7.3% in the adult polyp, and few cells are lost via apoptosis (less than 1.5%).

The second highest proliferative tissue is the gastrodermis, of endodermal origin, which also displays the highest apoptotic index in early life stages (figure 3*d*). DNA synthesis rates in this cell layer vary between 3.8 and 11.1%, peaking in the developing primary polyp. Apoptotic indices peak in early metamorphosis and primary polyp (at about 5%), then drop to 1.5% in adult coral. These data indicate that developmental morphogenetic processes in the gastrodermis simultaneously involve coral cell apoptosis in the early life stages (planula to primary polyp), and proliferation peaking in the primary polyp.

During the chase, the pharynx maintains high proportions of BrdU-labelled cells, but with a twofold decrease in BrdU signal intensity, indicating that active cell division compensates for cells leaving the pharynx area (figure 4*a*,*b*). The duration of the cell cycle is not known for scleractinian coral cells and few data are available for other cnidarian species. In *Hydra* sp. the cell cycle has been estimated to last 3–4 days, up to 7 days for epithelial cells and 8.5 days for gastrodermal cells [21–23]. In our study, the twofold dilution of BrdU-labelling over a 2 days chase suggests a shorter cell cycle compared with *Hydra*, lasting about 2 days for the coral epithelial cells from the pse and pharynx

areas. Further flow cytometry experiments would shed more light on cell cycling times in scleractinian corals. In this study, we show that BrdU-labelled cells accumulate in the pse of the oral tissue and also in the calicodermis of the aboral tissue (figure 4*c–f*). Taken together, these results reveal cell movements, migrating away from the pharynx to the pse and calicodermis. Additional influx of cells to these tissue layers from the gastrodermis is also possible, as this epithelium is the second most proliferative tissue in the primary polyp.

These results are consistent with our earlier findings in another scleractinian species, in which the pse (including the pharynx area) was also observed to be the most proliferative tissue in adult polyps, followed by the gastrodermis [8]. Spatial patterns of cell division observed in *S. pistillata* are similar to patterns reported for another anthozoan, the sea anemone *Nematostella vectensis*, where scattered cell division is observed along the entire body, with a hotspot of DNA synthesis identified in the pharynx [19,24]. More restricted proliferation patterns are present in hydrozoans. For example, in the freshwater *Hydra* polyp, proliferating cells are restricted to the body column, in which there is constant renewal of cells and migration to the apical and basal end of the polyp [16,22]. In the marine *Clytia hemisphaerica*, cell division of interstitial i-cells occurs in the epithelium at the tentacle base, from which cells migrate and differentiate into mature nematocysts mounted at the tip of tentacles [25].

(b) Cells in the skeletogenic calicodermis are non-cycling despite rapid growth of early life stages

The calicodermis appears to be essentially a non-proliferative epithelium (less than 2.5% of BrdU-positive cells), with non-cycling, terminally differentiated cells that are, however, actively producing skeleton (electronic supplementary material, figure S2). Cellular control of the coral biomineralization process has been proposed to involve highly localized proliferation or metabolic activity in the calicodermis [26]. Here, we demonstrate that active skeletal accretion is not associated with locally increased cellular proliferation in the overlying calicodermis. Moreover, our chase results indicate influx into the calicodermis of labelled cells from more proliferative reservoirs, primarily the pharynx and gastrodermis of the developing polyp. The exact migration pathway and number of divisions, from precursor cell until differentiated calicoblast, remains to be established. However, the BrdU signal intensity in calicoblast nuclei during the chase is lower by a factor of 2 to 4 compared with nuclei in more proliferative areas, which suggests one to two divisions during cell migration to the calicodermis. Correspondingly large standard deviations of the BrdU signal intensity in the calicodermis (figure 4*f*) indicate asynchronous cycling of the incoming cells. Migration may occur via displacement of epithelial cells in the pse, as in the *Hydra* body column [22], or through the mesenteries that connect the pharynx to the polyp basal floor [15,27].

The longevity of cells in quiescent calicodermis remains unclear. The calicodermis of the developing primary polyp is characterized by low rates of cell death via apoptosis (less than 3% TUNEL-positive nuclei). However, the transient accumulation, observed at 2 days into the chase, of BrdU-labelled cells imported from more proliferative reservoirs is followed by return to the initial low level at 64 h (figure 4*c*), indicating cell loss via a pathway different from apoptotic cell death. Future experiments with autophagy markers would shed more light on these processes; autophagy is known to be an important process in vertebrate development [28].

(c) Differential control of symbiont population by the host cells, depending on life stage

Constant dinoflagellate-to-gastrodermal cell ratio during metamorphosis indicates that the symbiont population is controlled by the host from the earliest life stages. In adult corals, it is known that a steady-state symbiont/host cell ratio is maintained through processes involving inorganic nutrient limitation (pre-mitotic control) and expulsion or cell death (post-mitotic control via autophagy or apoptosis) [2,28,29]. The dinoflagellate-to-gastrodermal cell ratio we observed through metamorphosis and development of *S. pistillata* was in the range 0.05–0.10 (figure 5*d*), with high variability in adult polyps reflecting high spatial heterogeneity of dinoflagellate abundance at colony level. This ratio is lower than the 0.15 ratio observed in adult *Acropora millepora* corals, but far above the ratio of bleached corals (0.005) [30]. The mitotic index we observed at all life stages is in agreement with values reported in adult scleractinian corals, typically being around or slightly below 5% [2]. However, the BrdU-labelling index was consistently higher for dinoflagellates compared with coral host (figure 5*a*), indicating that, early in development, the cell cycling activity of the endosymbionts surpasses that of the host cells.

During our experiments, inorganic nutrient concentrations in Eilat seawater were low, corresponding to an oligotrophic environment, and thus could not be responsible for the observed high *Symbiodinium* proliferation rates. The stability of dinoflagellate-to-gastrodermal cell ratio (figure 5*d*), despite higher DNA synthesis rates of endosymbionts (figure 5*a*), implies host regulation via post-mitotic control mechanisms. In planulae and during early metamorphosis, our results show that apoptosis is not the main endosymbiont regulation process, but that programmed cell death becomes essential for symbiont density regulation in the primary polyp and, to a lesser degree, in adult polyps (figure 5*c*). In planulae of *S. pistillata*, degradation of dinoflagellates has been reported [29] as well as release of symbionts into the water column [9]. Autophagy might also be involved in host regulation of the dinoflagellate population at early life stages, as it is known to be involved in adult coral bleaching [30]. Pre-mitotic control by host of dinoflagellate proliferation may be established only at the adult stage, when nutrient limitation and recycling mechanisms in the coral holobiont become fully developed [2].

5. Conclusion

This study has clearly identified the pharynx and gastrodermis as the most proliferative areas in the developing scleractinian polyp. Coral skeletal deposition does not involve proliferation of cells in the calicodermis, even during rapidly growing early life stages. Furthermore, our observations reveal an ontogenic succession of post-mitotic control mechanisms of the endosymbiotic dinoflagellate population density during host early development.

Data accessibility. The supporting datasets are summarized in the electronic supplementary material, tables SI–SV, and have been uploaded in the Dryad repository under the accession number http://dx.doi.org/10.5061/dryad.d9v45.

Authors' contributions. A.L., I.D.-C. and A.M. designed the experiment. A.L. carried out the experiments. A.P. and A.L. statistically analysed the data. All authors contributed to drafting and editing the manuscript.

Competing interests. We have no competing interests.

Funding. A.L. was funded by ERC Advanced grant no. 246749 'BIO-CARB' to A.M. Field labelling experiments, conducted at the marine station of the Inter-University Institute in Eilat, Israel, were funded through European ASSEMBLE call 6 programme CORALCELLPROLIF to I.D.-C., with additional grants from the MNHN programmes ATM 'Biomineralizations' and 'Formes'.

Acknowledgements. The PT-BIOP platform at EPFL Lausanne is acknowledged for access to and help with fluorescence microscopy. The PtME platform at MNHN is acknowledged for access to microtome and scanning electron microscope (electronic supplementary material, figure S2). We thank Shakib Djediat and Nicolas Rabet for discussions and Morgane Buet for drawing figure 1.

References

1. Stolarski J, Kitahara MV, Miller DJ, Cairns SD, Mazur M, Meibom A. 2011 The ancient evolutionary origins of Scleractinia revealed by azooxanthellate corals. *BMC Evol. Biol*. **11**, 316. (doi:10.1186/1471-2148-11-316)
2. Davy SK, Allemand D, Weis VM. 2012 Cell biology of Cnidarian-dinoflagellate symbiosis. *Microbiol. Mol. Biol. Rev*. **76**, 229–261. (doi:10.1128/MMBR.05014-11)
3. Falkowski PG, Dubinsky Z, Muscatine L, McCloskey L. 1993 Population control in symbiotic corals. *BioScience* **43**, 606–611. (doi:10.2307/1312147)
4. Pernice M, Dunn SR, Miard T, Dufour S, Dove S, Hoegh-Guldberg O. 2011 Regulation of apoptotic mediators reveals dynamic responses to thermal stress in the reef building coral *Acropora millepora*. *PLoS ONE* **6**, e16095. (doi:10.1371/journal.pone.0016095)
5. Kvitt H *et al.* 2015 Breakdown of coral colonial form under reduced pH conditions is initiated in polyps and mediated through apoptosis. *Proc. Natl Acad. Sci. USA* **112**, 2082–2086. (doi:10.1073/pnas.1419621112)
6. D'Angelo C, Smith EG, Oswald F, Burt J, Tchernov D, Wiedenmann J. 2012 Locally accelerated growth is part of the innate immune response and repair mechanisms in reef-building corals as detected by green fluorescent protein (GFP)-like pigments. *Coral Reefs* **31**, 1045–1056. (doi:10.1007/s00338-012-0926-8)
7. Yasuda N, Hidaka M. 2012 Cellular kinetics in growth anomalies of the scleractinian corals *Porites australiensis* and *Montipora informis*. *Dis. Aquat. Organ*. **102**, 1–11. (doi:10.3354/dao02530)
8. Lecointe A, Cohen S, Gèze M, Djediat C, Meibom A, Domart-Coulon I. 2013 Scleractinian coral cell proliferation is reduced in primary culture of suspended multicellular aggregates compared to polyps. *Cytotechnology* **65**, 705–724. (doi:10.1007/s10616-013-9562-6)
9. Rinkevich B, Loya Y. 1979 The reproduction of the Red Sea coral *Stylophora pistillata*. II. Synchronization in breeding and seasonality of planulae shedding. *Mar. Ecol. Prog. Ser*. **1**, 145–152. (doi:10.3354/meps001145)
10. Vandermeulen JH, Watabe N. 1973 Studies on reef corals. I. Skeleton formation by newly settled planula larva of *Pocillopora damicornis*. *Mar. Biol*. **23**, 47–57. (doi:10.1007/BF00394111)
11. Gilis M, Meibom A, Domart-Coulon I, Grauby O, Stolarski J, Baronnet A. 2014 Biomineralization in newly settled recruits of the scleractinian coral *Pocillopora damicornis*. *J. Morphol*. **275**, 1349–1365. (doi:10.1002/jmor.20307)
12. Byler KA, Carmi-Veal M, Fine M, Goulet TL. 2013 Multiple symbiont acquisition strategies as an adaptive mechanism in the coral *Stylophora pistillata*. *PLoS ONE* **8**, e59596. (doi:10.1371/journal.pone.0059596)
13. Santos SR, Toyoshima J, Kinzie RAIII. 2009 Spatial and temporal dynamics of symbiotic dinoflagellates (*Symbiodinium*: Dinophyta) in the perforate coral *Montipora capitata*. *Galaxea J. Coral Reef Stud*. **11**, 139–147. (doi:10.3755/galaxea.11.139)
14. Wilkerson FP, Kobayashi D, Muscatine L. 1988 Mitotic index and size of symbiotic algae in Caribbean Reef corals. *Coral Reefs* **7**, 29–36. (doi:10.1007/BF00301979)
15. Peters EC. 2016 Anatomy. In *Diseases of coral* (eds CM Woodley, CA Downs, AW Bruckner, JW Porter, SB Galloway), pp. 85–107. New York, NY: John Wiley & Sons, Inc.
16. David CN, Campbell RD. 1972 Cell cycle kinetics and development of *Hydra Attenuata* I. Epithelial cells. *J. Cell Sci*. **11**, 557–568.
17. Plickert G, Kroiher M, Munck A. 1988 Cell proliferation and early differentiation during embryonic development and metamorphosis of *Hydractinia echinata*. *Development* **103**, 795–803.
18. Chera S, Ghila L, Dobretz K, Wenger Y, Bauer C, Buzgariu W, Buzgariu W, Martinou J-C, Galliot B. 2009 Apoptotic cells provide an unexpected source of Wnt3 signaling to drive *Hydra* head regeneration. *Dev. Cell*. **17**, 279–289. (doi:10.1016/j.devcel.2009.07.014)
19. Passamaneck YJ, Martindale MQ. 2012 Cell proliferation is necessary for the regeneration of oral structures in the anthozoan cnidarian *Nematostella vectensis*. *BMC Dev. Biol*. **12**, 34. (doi:10.1186/1471-213X-12-34)
20. Fransolet D, Roberty S, Herman A-C, Tonk L, Hoegh-Guldberg O, Plumier J-C. 2013 Increased cell proliferation and mucocyte density in the sea anemone *Aiptasia pallida* recovering from bleaching. *PLoS ONE* **8**, e65015. (doi:10.1371/journal.pone.0065015)
21. Bosch TC, David CN. 1984 Growth regulation in *Hydra*: relationship between epithelial cell cycle length and growth rate. *Dev. Biol*. **104**, 161–171. (doi:10.1016/0012-1606(84)90045-9)
22. Holstein TW, Hobmayer E, David CN. 1991 Pattern of epithelial cell cycling in *Hydra*. *Dev. Biol*. **148**, 602–611. (doi:10.1016/0012-1606(91)90277-A)
23. Govindasamy N, Murthy S, Ghanekar Y. 2014 Slow-cycling stem cells in *Hydra* contribute to head regeneration. *Biol Open* **3**, 1236–1244. (doi:10.1242/bio.201410512).
24. Singer II. 1971 Tentacular and oral-disc regeneration in the sea anemone, *Aiptasia diaphana*. 3. Autoradiographic analysis of patterns of tritiated thymidine uptake. *J. Embryol. Exp. Morphol*. **26**, 253–270.
25. Denker E, Manuel M, Leclère L, Le Guyader H, Rabet N. 2008 Ordered progression of nematogenesis from stem cells through differentiation stages in the tentacle bulb of *Clytia hemisphaerica* (Hydrozoa, Cnidaria). *Dev. Biol*. **315**, 99–113. (doi:10.1016/j.ydbio.2007.12.023)
26. Tambutté E, Allemand D, Zoccola D, Meibom A, Lotto S, Caminiti N, Tambutté S. 2007 Observations of the tissue-skeleton interface in the scleractinian coral *Stylophora pistillata*. *Coral Reefs* **26**, 517–529. (doi:10.1007/s00338-007-0263-5)
27. Seipel K, Schmid V. 2006 Mesodermal anatomies in cnidarian polyps and medusae. *Int. J. Dev. Biol*. **50**, 589. (doi:10.1387/ijdb.062150ks)
28. Aburto MR, Hurlé JM, Varela-Nieto I, Magariños M. 2012 Autophagy during vertebrate development. *Cells* **1**, 428–448. (doi:10.3390/cells1030428)
29. Titlyanov EA, Titlyanova TV, Loya Y, Yamazato K. 1998 Degradation and proliferation of zooxanthellae in planulae of the hermatypic coral *Stylophora pistillata*. *Mar. Biol*. **130**, 471–477. (doi:10.1007/s002270050267)
30. Dunn SR, Schnitzler CE, Weis VM. 2007 Apoptosis and autophagy as mechanisms of dinoflagellate symbiont release during cnidarian bleaching: every which way you lose. *Proc. R. Soc. B* **274**, 3079–3085. (doi:10.1098/rspb.2007.0711)

Data Supplement - Lecointe et al 2016 prsb Published 18 May 2016.DOI: 10.1098/rspb.2016.0206

- Figure S1 - Imaging method for quantification of BrdU-labeled nuclei immunodetected in the coral tissue layers. (A) Toluidine blue semi-thin section (1µm) of S. pistillata adult polyp. (B-E) BrdU is detected with Alexa-594 (red) colocalized with DAPI-stained nuclei (blue) in (B) the corresponding serial transverse section from the same adult polyp , (C) longitudinal section from a primary polyp, oriented through the highly labeled pharynx area (cell layers are outlined in white). (D-E) Magnified view highlighting in (D) the pharynx with (a) unlabeled nuclei (b) BrdU-labeled nuclei, and in (E) the gastrodermis with (c) a dinoflagellate cell with unlabeled nuclei (d) a dinoflagellate cell with BrdU labeled nuclei. t: tentacle, gc: gastric cavity, pse: pseudostratified epithelium, og: oral gastrodermis, ag: aboral gastrodermis, cal: calicodermis, sk: decalcified skeleton. Alexa-594 labeling which does not co-localize to nuclei is considered an artefact (* in skeletal space)

- Figure S2 - Skeleton deposition during metamorphosis. (A) Scanning electron micrograph of skeleton already deposited by Stylophora pistillata at the 'early metamorphosis' stage. (B) Magnified view of a growing septa.

- Figure S3 - Chase of the BrdU labeling in the gastrodermis (A) BrdU-labeling index in the primary polyp at the start, 48 h, and 64 h into the chase in normal seawater. Data are expressed as boxplots (c.f. M&M in main text) for the dinoflagellates (dark gray) and the gastrodermal coral cells (light gray). A star indicates statistical difference between gastrodermal cells and dinoflagellates (glm, p-value<0.05). (B) Dilution of BrdU signal intensity for the gastrodermal coral cells and (C) for the dinoflagellates. A star indicates a statistical difference between two consecutive time points (Kruskal-Wallis and pairwise Wilcoxon test, p-value<0.05

- Supplementary data tables I, II, II, IV, V - Detailed data for each end point assay.

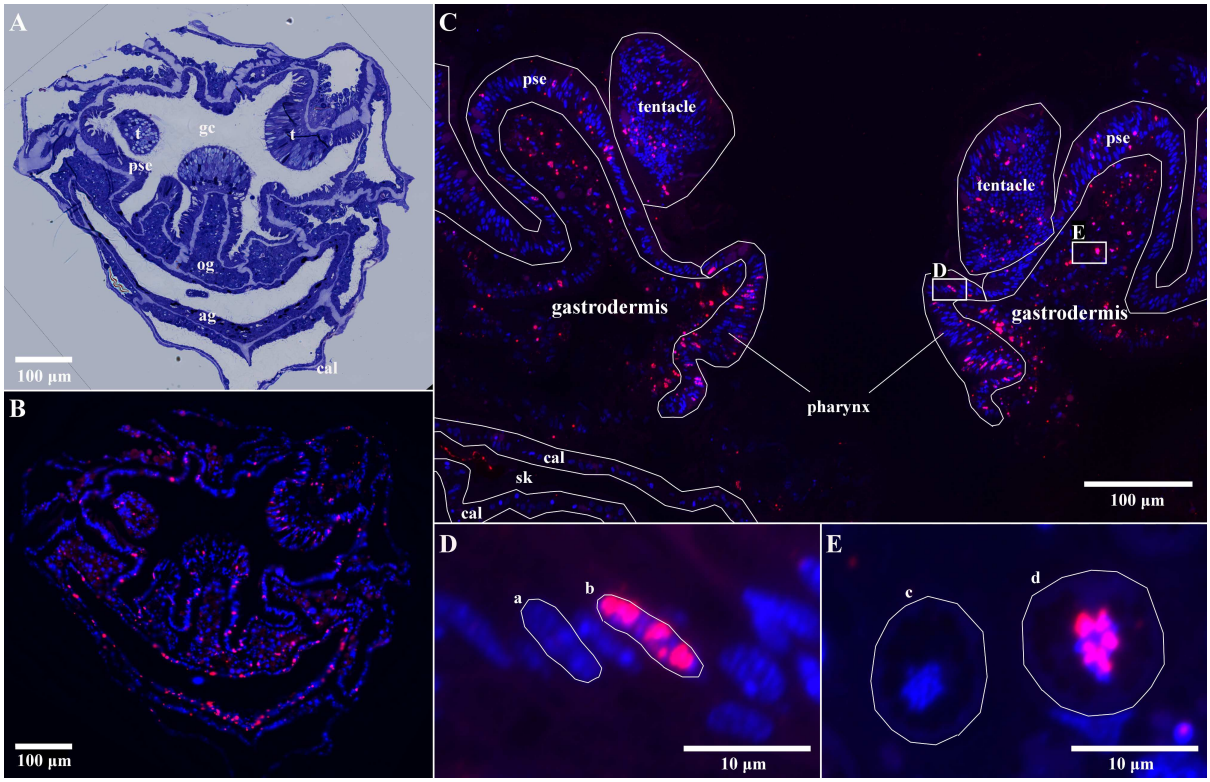
A
gc
t
t
pse
og
ag
cal
100 µm
B
100 µm
C
pse
tentacle
pse
tentacle
E
D
gastrodermis
gastrodermis
pharynx
cal
sk
cal
100 µm
D
a
b
10 µm
E
c
d
10 µm

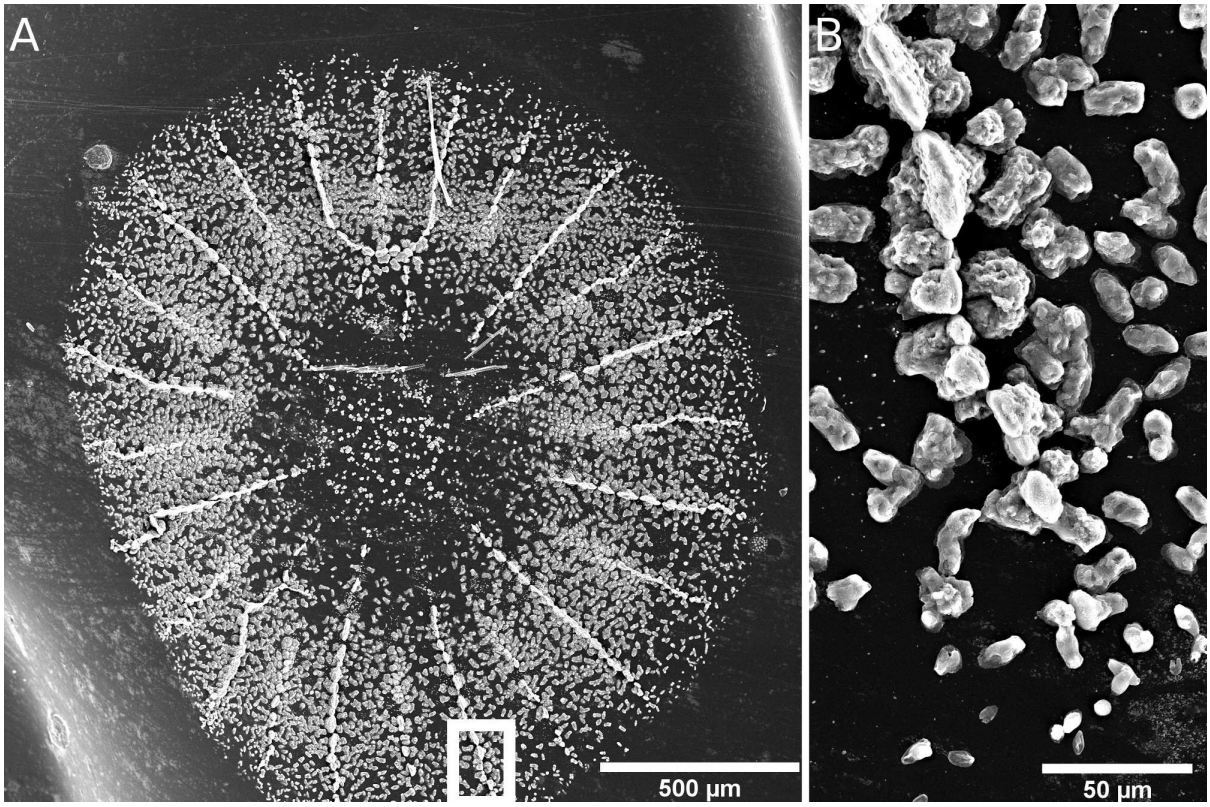
A
500 µm
B
50 µm

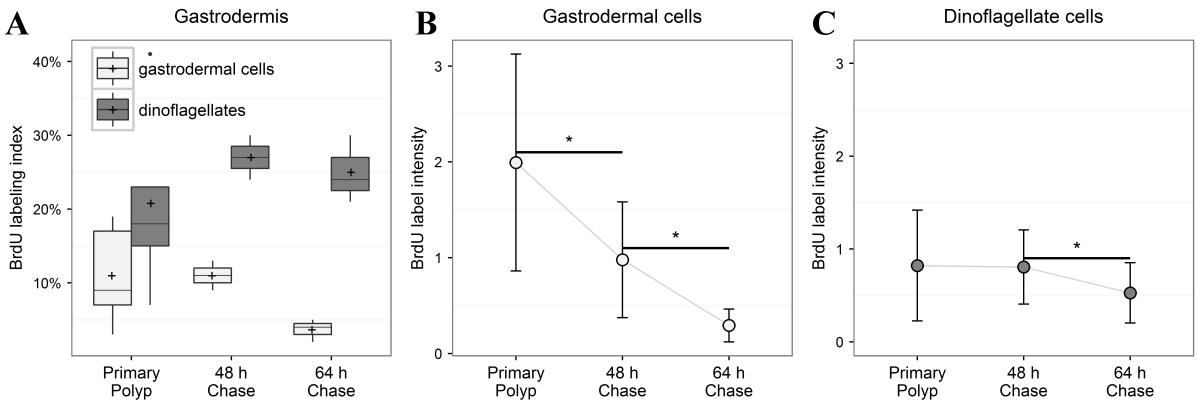
A
Gastrodermis
gastrodermal cells
dinoflagellates
BrdU labeling index
40%
30%
20%
10%
Primary Polyp
48 h Chase
64 h Chase
B
Gastrodermal cells
BrdU label intensity
3
2
1
0
*
*
Primary Polyp
48 h Chase
64 h Chase
C
Dinoflagellate cells
BrdU label intensity
3
2
1
0
*
Primary Polyp
48 h Chase
64 h Chase

Table I: BrdU 24h-labeling index of coral and dinoflagellate cells

	Planula			Early metamorphosis			Primary polyp			Adult		
Tissue	mean	SD	nuclei number	mean	SD	nuclei number	mean	SD	nuclei number	mean	SD	nuclei number
pharynx	2,3%	± 2,2%	5214	2,4%	± 1,2%	2575	19,3%	± 7,3%	1921	5,5%	± 2,0%	3455
pseudostratified epithelium	1,4%	± 1,0%	64810	2,9%	± 2,6%	46583	2,9%	± 2,5%	27176	7,3%	± 1,6%	5896
calicodermis	0,4%	± 0,7%	10972	2,2%	± 3,8%	14498	0,4%	± 0,4%	11362	2,5%	± 2,2%	345
gastrodermis	5,7%	± 4,4%	46796	4,7%	± 1,5%	12713	11,1%	± 6,7%	24513	3,8%	± 1,6%	7885
dinoflagellates	29,5%	± 20,9%	1793	10,0%	± 15,2%	669	20,8%	± 12,8%	1204	9,8%	± 4,8%	737

nuclei pooled from 2-6 sections per replicate, 3-5 replicates per timepoint

Table II: Apoptotic index of coral and dinoflagellate cells

	Planula			Early metamorphosis			Primary polyp			Adult		
Tissue	mean	SD	nuclei number	mean	SD	nuclei number	mean	SD	nuclei number	mean	SD	nuclei number
pharynx	0,6%	± 0,4%	2121	1,1%	± 0,7%	1496	2,5%	± 2,1%	1053	0,5%	± 0,4%	1168
pseudostratified epithelium	0,6%	± 0,4%	7021	0,7%	± 0,5%	8219	1,0%	± 0,9%	5992	1,4%	± 1,1%	1300
calicodermis	1,5%	± 1,5%	2139	1,4%	± 1,2%	4124	1,9%	± 1,1%	2493	2,6%	± 0,7%	657
gastrodermis	3,3%	± 2,5%	4675	5,1%	± 2,4%	5136	4,1%	± 4,3%	3927	1,5%	± 0,7%	2120
dinoflagellates	12,8%	± 6,7%	172	11,3%	± 5,6%	149	34,5%	± 27,8%	209	27,7%	± 11,6%	172

nuclei pooled from 1-4 sections per replicate, 3 replicates per timepoint

Table III: BrdU labeling index during the chase experiment

	Primary polyp (t0)			48 h Chase			64 h Chase		
Tissue	mean	SD	nuclei number	mean	SD	nuclei number	mean	SD	nuclei number
pharynx	19,3%	± 7,3%	1921	19,8%	± 4,4%	1756	11,4%	± 6,6%	2848
pseudostratified epithelium	2,9%	± 2,5%	27176	15,6%	± 5,7%	6886	2,3%	± 2,4%	10534
calicodermis	0,4%	± 0,4%	11362	2,9%	± 2,5%	5188	1,0%	± 1,0%	2131
gastrodermis	11,1%	± 6,7%	24513	10,9%	± 2,8%	9032	3,5%	± 1,7%	6563
dinoflagellates	20,8%	± 12,8%	1204	26,7%	± 4,4%	656	25,1%	± 4,7%	365

nuclei pooled from 4-6 sections per replicate, 2-5 replicates per time-point

Table IV: Nuclei BrdU-labeling intensity

	Primary polyp			48 h Chase			64 h Chase		
Tissue	mean	SD	nuclei number	mean	SD	nuclei number	mean	SD	nuclei number
pharynx	0,94	± 0,40	30	0,36	± 0,12	30	0,18	± 0,06	30
pseudostratified epithelium	1,04	± 0,45	54	0,44	± 0,21	60	0,26	± 0,10	37
calicodermis	0,57	± 0,46	19	0,40	± 0,12	21	0,28	± 0,08	7
gastrodermis	1,99	± 1,13	59	0,98	± 0,60	60	0,30	± 0,17	58
dinoflagellates	0,8	± 0,6	30	0,8	± 0,4	30	0,5	± 0,3	30

7-60 nuclei measured per replicate, 3 replicates per time-point

Table V: Mitotic index of dinoflagellates

	Planula			Early metamorphosis			Primary polyp			Adult		
	mean	SD	nuclei number	mean	SD	nuclei number	mean	SD	nuclei number	mean	SD	nuclei number
dinoflagellates	1,6%	± 0,7%	1978	2,2%	± 1,2%	1168	6,3%	± 2,3%	1424	2,4%	± 0,9%	1196

mitotic index evaluated in 2-8 sections per replicate, 3 replicates per time-point